Three-dimensional analysis of water infiltration into the Gouhou rockfill dam using saturated–unsaturated seepage theory

Qun Chen and L.M. Zhang

Abstract: The Gouhou Dam was a concrete-faced rockfill dam built in a steep canyon that collapsed in 1993 due to internal erosion during the initial reservoir filling. In this paper, the process of water infiltration into the originally unsaturated rockfill dam is studied using three-dimensional saturated–unsaturated seepage theory. The three-dimensional characteristics of seepage through the dam bounded by steep abutments, the effect of material anisotropy, and the effect of rockfill stratifications are studied. The three-dimensional results are compared with those from two-dimensional analyses. The three-dimensional simulations show that seepage water flows faster and the hydraulic gradients are greater near the abutment boundary in the dam. As such, the evolution of the seepage failure in the three-dimensional cases is faster than that in the two-dimensional analyses, and the two-dimensional analyses will underestimate the risk of seepage failure, particularly near the abutment boundary. If the materials in the dam were uniform, the reservoir water would infiltrate into the dam along a downward flow path towards the riverbed, and not exit from the surface on the downstream slope. Increasing the horizontal coefficient of permeability of the rockfill increases the infiltration velocity, but the material anisotropy does not appreciably change the infiltration pattern. Stratifications in the rockfill, however, cause the seepage water to advance more quickly in the horizontal direction along the interface between the sandwich layer and the rockfill, thus increasing the possibility of seepage failure.

Key words: seepage, seepage failure, rockfill dam, unsaturated soils, wetting front, numerical analysis.

Résumé : Le barrage Gouhou était un barrage d'enrochements avec face amont en béton construit dans un canyon profond. Le barrage s'est effondré en 1993 lors de la mise en eau du réservoir par suite d'une érosion interne. Au moyen de la théorie d'infiltration tridimensionnelle saturée – non saturée, on étudie dans cet article le processus d'infiltration d'eau dans ce barrage d'enrochements à l'origine non saturés. On a étudié les caractéristiques tridimensionnelles de l'infiltration à travers le barrage construit entre des appuis abruptes, de même que l'effet de l'anisotropie du matériau, et l'effet des stratifications de l'enrochement. On compare les résultats tridimensionnels avec ceux obtenus par des analyses bidimensionnelles. Les simulations tridimensionnelles montrent que l'eau d'infiltration coule plus rapidement et les gradients hydrauliques sont plus grands près des appuis dans le barrage. Ainsi, l'évolution de la rupture par infiltration dans les cas tridimensionnels est plus rapide que dans les analyses bidimensionnelles, et les analyses bidimensionnelles vont sous-estimer le risque de rupture par infiltration, particulièrement près de la surface des appuis. Si les matériaux dans le barrage étaient uniformes, l'eau du réservoir s'infiltrerait dans le barrage le long du cheminement de l'écoulement vers le bas, soit vers le lit de la rivière, et ne sortirait pas de la surface du parement aval. L'accroissement du coefficient de perméabilité horizontal de l'enrochement augmente la vitesse d'infiltration, mais l'anisotropie du matériau ne change pas appréciablement le schéma d'infiltration. Cependant, les stratifications dans l'enrochement causent une progression plus rapide de l'eau d'infiltration dans la direction horizontale le long de l'interface entre les couches intercalées dans l'enrochement, ce qui accroît la possibilité de rupture par infiltration.

Mots clés : infiltration, rupture par infiltration, barrage en enrochements, sols non saturés, front de saturation, analyse numérique.

[Traduit par la Rédaction]

Introduction

The Gouhou Dam was a 71 m high concrete-faced rockfill dam located in Gonghe County, Qinghai Province, China. The design, construction, operation, and failure of the dam have been reported by the Gouhou Dam Failure Investigation Team (1996). The rockfill dam was built in a steep canyon directly above a 10 m thick sandy gravel layer overlying

Received 7 January 2005. Accepted 20 December 2005. Published on the NRC Research Press Web site at http://cgj.nrc.ca on 6 April 2006.

Q. Chen. State Key Laboratory of Hydraulics and Mountain River Engineering, School of Hydraulic and Hydroelectric Engineering, Sichuan University, Chengdu, Sichuan, China.
L.M. Zhang.[1] Department of Civil Engineering, Hong Kong University of Science and Technology, Clear Water Bay, Hong Kong.

[1]Corresponding author (e-mail: cezhangl@ust.hk).

 doi:10.1139/T06-011

Fig. 1. Gouhou Dam: (*a*) maximum cross section profile; (*b*) upstream elevation view (after Gouhou Dam Failure Investigation Team 1996). All units in metres.

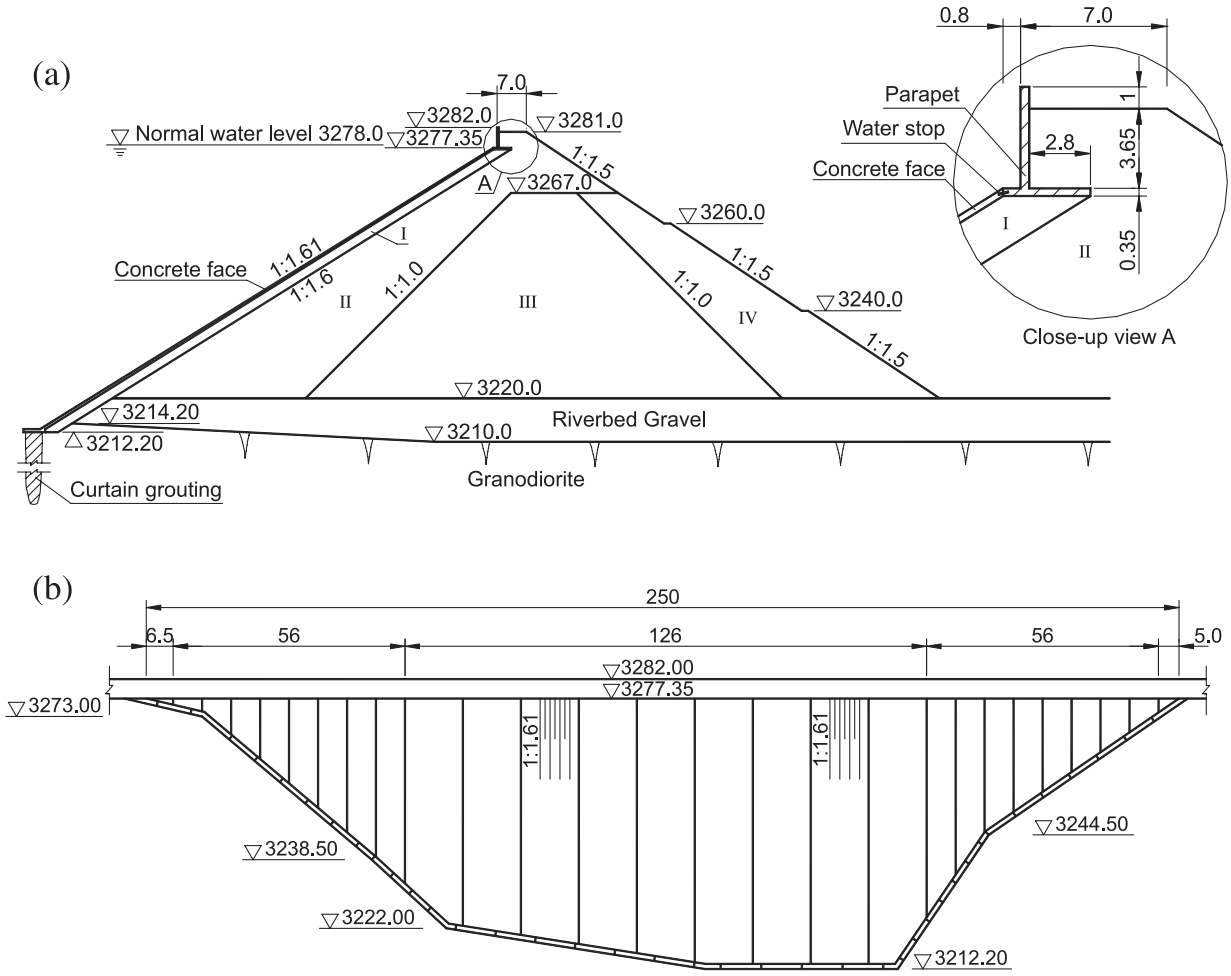

bedrock. The dam crest, at an elevation of 3281 m, was 265 m long and 7 m wide. The design, normal, and check water levels were all 3278 m, and the corresponding reservoir volume was 3.1 million cubic metres. The maximum cross section and the upstream elevation view of the dam are shown in Fig. 1. The rockfill was divided into four zones. Zone I was the transition material supporting the concrete face, and zones II–IV were the main rockfill. The upstream and downstream dam slopes were 1:1.6 and 1:1.5, respectively.

According to forensic investigations by the Gouhou Dam Failure Investigation Team (1996), the reservoir water level rose continuously from 3261.0 m on 14 July 1993 to 3277.0 m at 12:00 on 27 August. The reservoir water then started to flow into the dam from the joint between the bottom platform of the parapet wall and the concrete face (see close-up view A in Fig. 1). At about 20:00 on the same day, seepage water exited from the downstream slope of the dam at elevation 3260 m, triggering a seepage failure of the dam. The dam was breached in less than 3 h. The failure of the dam caused flooding of a town downstream from the dam and 288 casualties.

The Gouhou Dam was one of many dam failures related to seepage during reservoir filling. According to the available statistics (Fell et al. 1992; Foster et al. 2002), other than overtopping, internal erosion and piping caused by seepage are the primary causes of failures and incidents in embankment dams. Teton Dam in the United States failed in 1976 due to erosion of the core material near the abutment during initial reservoir filling (USCOLD 1988). Panshet Dam in India failed in 1961 due to piping when the first phase was near completion (Singh and Varshney 1995). Abutment seepage was also the cause of some additional incidents at earth or rockfill dams, such as Clear Branch Dam, East Branch Dam, and Navajo Dam (USCOLD 1988).

Seepage analyses are an important tool to assess the susceptibility of seepage failure in dams and to study hydraulic conditions for analyzing the stability of dam slopes. Early transient seepage analyses were based on seepage theory for saturated soils, and the determination of the free surface was the key problem. Finite element methods involving a variable mesh procedure (Dvinoff and Harr 1971; Desai 1972; Bathe and Khoshagoftaar 1979), finite difference methods involving a Boiocchi-type transformation method (Gupta et al. 1986), and boundary element methods (Chang 1987) have been used to solve for the location of the free surface. Freeze (1971) and Neuman (1972) are the foremost researchers who considered the unsaturated properties of the soil for transient seepage analysis of dams. Later, two-dimensional transient seepage analyses using saturated–

unsaturated seepage theory were conducted to consider initial filling of various reservoirs (Lam et al. 1987; Ng and Small 1995; Chen et al. 2005) and water-level fluctuations in front of dams (Aral and Maslia 1983; Lam et al. 1987).

For dams built in narrow valleys, three-dimensional effects are likely significant, and two-dimensional simplifications may not be consistent with field conditions. To consider three-dimensional effects in seepage through dams, Gupta et al. (1986), Xie et al. (2001), and other investigators conducted three-dimensional analyses based on saturated seepage theory. Freeze (1971) presented a three-dimensional analysis of flow through earth dams that included unsaturated soil domains. The three-dimensional analysis was a steady-state analysis and the flow exit point was determined by a trial-and-error method. Recently, some three-dimensional analyses (Russo et al. 1998; Ng et al. 2001; Zhou et al. 2002) were performed to study rainfall infiltration into homogeneous soils and unsaturated soil slopes. Only limited studies have been reported, however, that consider three-dimensional reservoir water infiltration into originally unsaturated rockfill dams.

After the disastrous failure of the Gouhou Dam, several studies were conducted to determine the failure mechanisms (Chen and Zhao 1996; Liu and Miao 1996; Liu et al. 1998). Chen and Zhao (1996) analyzed the stability of the dam slope and conducted a two-dimensional steady-state seepage analysis using a saturated seepage theory. The dam was considered as a uniform and saturated structure, and the horizontal stratification of the rockfill was included by considering the embankment as an anisotropic material. Recently, Chen et al. (2005) conducted a two-dimensional transient seepage analysis of the Gouhou Dam using saturated–unsaturated seepage theory. The effect of material stratification on the seepage field of the dam was investigated. The dam was constructed in a steep valley, however. The ratio of the maximum length of the dam to the maximum width at the base of dam was only 1.1, and the ratio of the length of the dam to the height of the dam was only 3.6 (see Fig. 1). Three-dimensional characteristics of seepage flow through the dam are therefore likely to be significant.

The objective of this paper is to study the influence of three-dimensional geometrical characteristics associated with the Gouhou Dam on the infiltration of the reservoir water into the originally unsaturated rockfill using saturated–unsaturated seepage theory. By comparing the three-dimensional results with the results from two-dimensional analyses, the three-dimensional effects on the infiltration process can be investigated. In addition, the three-dimensional seepage pattern in the dam with material stratifications is illustrated, and the effect of material anisotropy on the flow pattern is studied.

Equations for saturated–unsaturated seepage

Darcy's law is considered valid for seepage in both saturated and unsaturated soils (Fredlund and Rahardjo 1993). The major differences between water flow in saturated and unsaturated soils are (*i*) the coefficient of permeability is not a constant but a function of the degree of saturation or matric suction in unsaturated soils, and (*ii*) the volumetric water content of an unsaturated soil can vary with time. The governing equation for water flow through an unsaturated soil can be obtained by introducing Darcy's law into the continuity equation. When the hydraulic properties of the soil are transversely anisotropic, the three-dimensional governing differential equation is as follows:

$$[1] \qquad \frac{\partial}{\partial x}\left(k_x \frac{\partial h}{\partial x}\right)+\frac{\partial}{\partial y}\left(k_y \frac{\partial h}{\partial y}\right)+\frac{\partial}{\partial z}\left(k_z \frac{\partial h}{\partial z}\right)=-\frac{\partial \theta_w}{\partial t}$$

where k_x, k_y, and k_z are the coefficients of permeability in the x, y, and z directions, respectively; h is the total head; θ_w is the volumetric water content; and t is the time.

Using two independent stress state variables (Fredlund and Morgenstern 1977), namely net normal stress ($\sigma - u_a$, where σ is the total normal stress and u_a is the pore-air pressure) and matric suction ($u_a - u_w$, where u_w is the pore-water pressure), to describe the stress state and volume changes, a simplified constitutive equation for the water phase of an isotropic unsaturated soil is (Lam et al. 1987)

$$[2] \qquad d\theta_w = \frac{\partial \theta_w}{\partial(\sigma - u_a)} d(\sigma - u_a) + \frac{\partial \theta_w}{\partial(u_a - u_w)} d(u_a - u_w)$$

If the net normal stress changes and deformations of the soil skeleton are ignored during the transient seepage process and the air phase is continuous in the soil, the time rate of volumetric water content change can be simplified as follows:

$$[3] \qquad \frac{\partial \theta_w}{\partial t} = -\frac{\partial \theta_w}{\partial \psi}\frac{\partial u_w}{\partial t}$$

where $\psi = u_a - u_w$ is the matric suction. Combining eqs. [1] and [3] and expressing the pore-water pressure in terms of the total head h, the governing differential equation for three-dimensional transient seepage can therefore be written as follows:

$$[4] \qquad \frac{\partial}{\partial x}\left(k_x \frac{\partial h}{\partial x}\right)+\frac{\partial}{\partial y}\left(k_y \frac{\partial h}{\partial y}\right)+\frac{\partial}{\partial z}\left(k_z \frac{\partial h}{\partial z}\right)=\gamma_w \frac{\partial \theta_w}{\partial \psi}\frac{\partial h}{\partial t}$$

where γ_w is the unit weight of water. According to eq. [4], the soil-water characteristic curve (i.e., the relationship between θ_w and ψ) and the permeability function are required to perform an analysis.

Three-dimensional transient seepage analysis of the Gouhou Dam

Solution algorithms

The finite element program SVFlux (SoilVision Systems Ltd. 2003) and a partial differential equation solver FlexPDE (PDE Solutions Inc. 2003) were used to study the three-dimensional reservoir water infiltration in the Gouhou rockfill dam. SVFlux is a comprehensive finite element program developed to simulate the movement of water and the distribution of pore-water pressure in two- and three-dimensional saturated or unsaturated domains. FlexPDE is a fully integrated partial differential equation solver combining several modules to provide a comprehensive problem-solving platform. It provides fully automated mesh genera-

Fig. 2. Simplified profile and boundary conditions for three-dimensional transient seepage analysis.

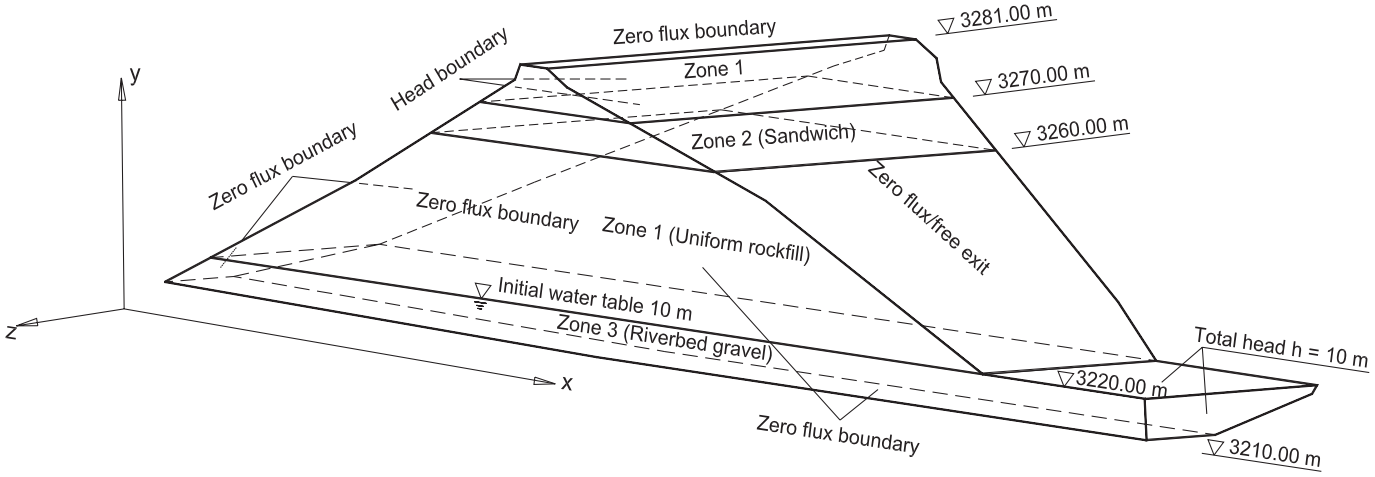

tion, automated mesh refinement, and automated time step refinement. A mesh-generation module in FlexPDE constructs a triangular mesh over an arbitrary two-dimensional domain. In a three-dimensional problem, the elements are extruded into tetrahedral meshes. Bilinear interpolation is used in three-dimensional problems to approximate a curved surface. Once the initial mesh has been constructed, FlexPDE will estimate the solution error and refine the mesh as necessary to meet the target accuracy. In time-dependent problems, an adaptive refinement process is applied to the initial values of the variables. The adaptive refinement feature is also used to refine any part of the mesh where the variables undergo rapid changes. FlexPDE will also apply a heuristic control on the time step used to track the evolution of the system.

Simulation cases and boundary conditions

The Gouhou Dam (Fig. 1*a*) was a zoned rockfill dam. The material zones differed only in the maximum grain sizes of the rockfill materials. There were few large boulders, so the dam was nearly uniform according to the results of an investigation of the remnants on both ends of the dam after failure (Gouhou Dam Failure Investigation Team 1996). Field investigations revealed some serious problems in the structure of the dam (Liu et al. 1998). First, the water stop between the concrete parapet wall and the concrete face was not working correctly for a long distance in the longitudinal direction, which left a concentrated seepage channel between the reservoir water and the rockfill. Second, because of the deformation of the rockfill, the concrete face separated from the transition zone material for several metres below the parapet wall. Third, the rockfill was seriously segregated, so stratifications of coarse and fine layers were present. The coarse layers were about 0.3–0.4 m thick and extended from the upstream face to the downstream face. The saturated coefficient of permeability of the coarse layers was as high as 0.02–0.44 m/s.

Considering the detailed structure of the dam, two simulation cases were considered for the three-dimensional transient seepage analysis. The simplified three-dimensional profile and boundary conditions are shown in Fig. 2. There are three primary material zones. Case I assumes a uniform rockfill dam with the concrete face being impervious below

Fig. 3. Average, lower and upper limits, and riverbed grain-size distribution curves of the rockfill materials.

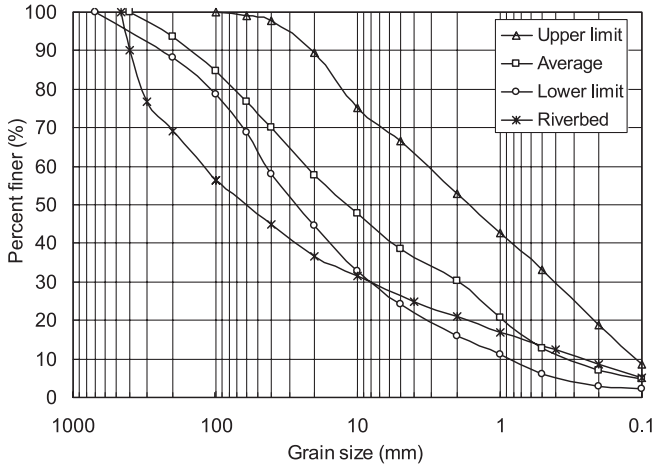

elevation 3260 m. The upper limit of the grain-size distribution of the rockfill (see Fig. 3) is taken as the material for zone 1 and zone 2 in this case. Zone 3 is the riverbed gravel in all cases. Case II includes a 10 m thick sandwich layer (zone 2) between elevations 3260 and 3270 m. The sandwich layers are represented by the lower limit (as shown in Fig. 3) of the rockfill based on samples taken from the field during construction and after dam failure. The average grain-size distribution (see Fig. 3) of the rockfill is taken as the material for zone 1. The simulation cases and the corresponding zoning and materials are listed in Table 1.

The initial groundwater table is assumed to lie at the base of the dam, and the riverbed is submerged. The matric suction is assumed to increase linearly with increase in elevation above the water table, but the maximum matric suction is limited to 14.2 kPa, which corresponds to the average suction of the rockfill at the average compaction water content of 3.5% during construction. The same initial conditions are applied to both simulation cases.

The boundary conditions for the two cases are shown in Fig. 2. It is assumed that the concrete face is impervious below elevation 3260 m but is ineffective above that elevation, in lieu of the defective water stop between the parapet wall

Fig. 4. Finite element discretization mesh of the three-dimensional analysis domain: (*a*) side view; (*b*) downstream view.

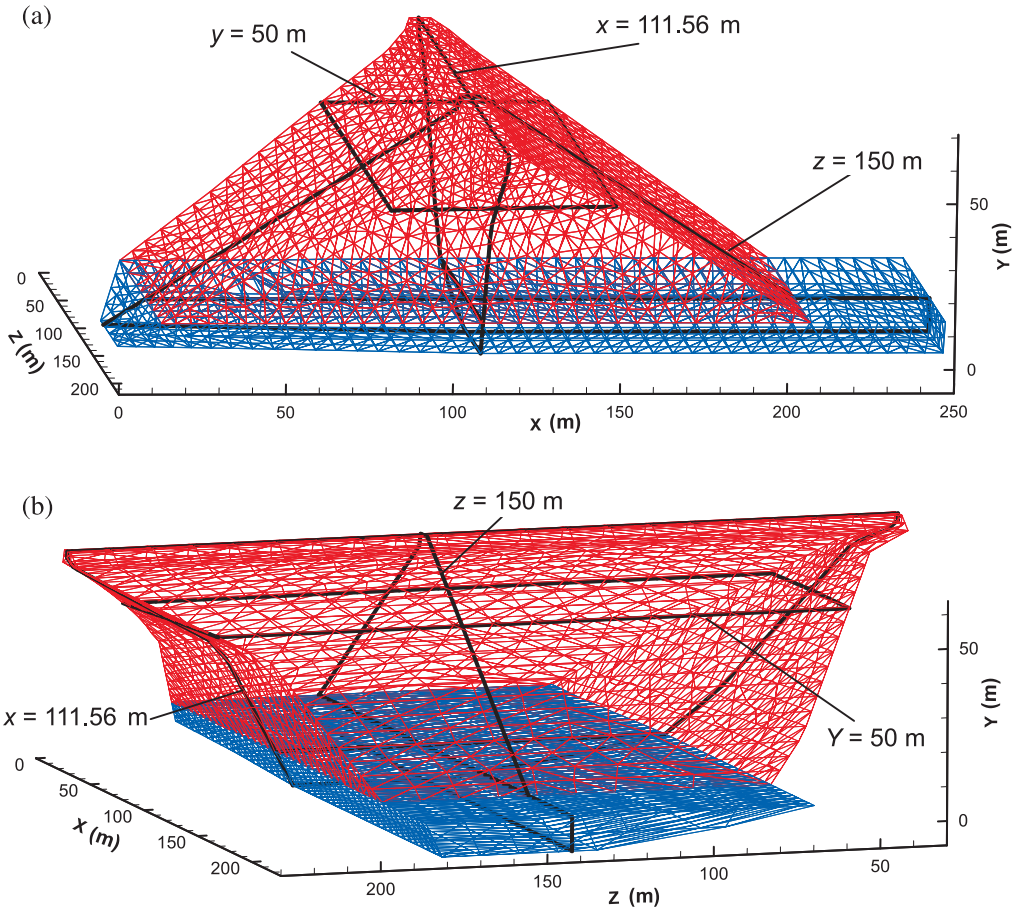

Table 1. Simulation cases and corresponding zone and material.

Zone	Material
Case I: homogeneous	
1	Upper limit of grain-size distribution of rockfill
2	Same as zone 1 material
3	Riverbed gravel
Case II: sandwich layer	
1	Average grain-size distribution of rockfill
2	Lower limit of grain-size distribution of rockfill
3	Riverbed gravel

and the concrete face, and the separation gap between the concrete face and the transition zone. Therefore, the boundary condition for the upstream slope surface of the dam is defined in two parts. The upper part (above elevation 3260 m) is a total head condition and the lower part (below elevation 3260 m) is a zero-flux condition. The total head condition is defined as a rising water level from elevation 3277 m (i.e., the elevation of the bottom plate of the parapet wall) to elevation 3277.3 m (i.e., the maximum water level before dam failure) within the first day and a constant water level of 3277.3 m afterwards. A zero-flux boundary is applied along the dam crest. The downstream slope is defined as a zero-flux boundary condition if the total head is less than the elevation head and a free outflow boundary otherwise (a "review" boundary, see SoilVision Systems Ltd. 2003). The initial water table is assumed to be the same as the rockfill base level (10 m), and the downstream boundary of the riverbed has a constant total head of 10 m. It is also assumed that the abutment rock along the canyon and the bedrock below the riverbed are impervious. The finite element mesh for the three-dimensional analysis is shown in Fig. 4.

Material properties

The average grain-size distribution curve and the lower and upper limits of the grain size of the rockfill samples obtained from laboratory tests are shown in Fig. 3 (Gouhou Dam Failure Investigation Team 1996). The range of the grain-size distributions of the rockfill is wide, indicating that there was significant segregation of the rockfill particles during construction. The grain-size distribution curve for the sandy gravel in the riverbed (zone 3 in Fig. 2) is also shown in Fig. 3. The index properties and the values of the saturated coefficient of permeability (listed in Table 2) of the four materials used in the seepage analyses are determined from laboratory tests of the rockfill of the Gouhou Dam (Gouhou Dam Failure Investigation Team 1996).

Two soil property functions, the soil-water characteristic curve and the permeability function, are required to solve the partial differential equation (eq. [4]) for the transient seepage analysis. In this paper, they were estimated following the procedures proposed by Fredlund et al. (1994, 2002). The estimated soil-water characteristic curves and the per-

Table 2. Index properties of the four materials used in the seepage analyses.

Material	Specific gravity, G_s	Initial water content, w (%)	Porosity, n (%)	Saturated coefficient of permeability, k_{sat} ($\times 10^{-5}$ m/s)
Upper limit of rockfill	2.68	3.5	0.21	2.2
Average of rockfill	2.68	3.5	0.21	11.6
Lower limit of rockfill	2.68	3.5	0.21	231.0
Riverbed gravel	2.71	12.3	0.27	7.4

Fig. 5. Estimated soil-water characteristic curves (*a*) and permeability functions (*b*) for the four soils.

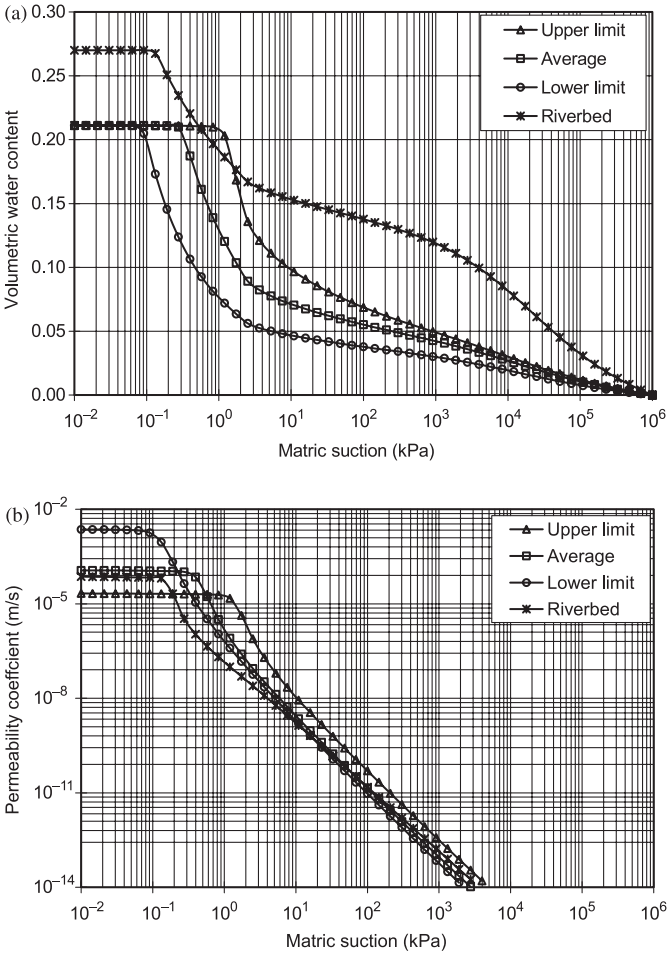

meability functions for the four soils are shown in Figs. 5*a* and 5*b*, respectively.

Three-dimensional seepage characteristics in the dam

Three sections, z = 150 m (the maximum cross section), y = 50 m (the horizontal section at elevation 3260 m), and x = 111.56 m (the longitudinal vertical section through the dam axis), were extracted from the three-dimensional domain for analysis to show the infiltration characteristics in each dimension of the Gouhou Dam (Fig. 4).

First, a uniform rockfill dam (case I) is studied assuming that there was no evident difference among the material zones. Figure 6 shows the evolution of the phreatic surface in the dam for case I. Water infiltrates into the dam gradually from the upper part of the upstream slope where the concrete face is defective. The wetting front develops downwards. Before the perched water table reaches the initial groundwater table in the riverbed, the whole dam rockfill is divided into two zones by the perched water table. One is the zone within the perched water table where the pore-water pressures are positive. The other is the unsaturated zone outside the perched water table where the pore-water pressures are negative. The perched water does not exit from the downstream slope, even after 9 days of infiltration.

Figure 7 shows the pore-water pressure contours in the cross section at z = 150 m at different times for case I. The contours with zero pore-water pressure represent the transient phreatic surfaces. The pore-water pressures decrease gradually from a maximum at elevation 3260 m on the upstream surface to zero at the perched water table. After 4.5 days, the bottom of the perched water table reaches the initial groundwater table in the riverbed, and a connected seepage channel from the upper portion of the upstream slope to the riverbed forms in the dam. The upstream dam slope is gradually saturated by the infiltrated water (Fig. 7*c*), and only a small area near the upstream slope surface remains unsaturated on the 9th day, as shown in Fig. 7*d*.

The evolution of seepage flow obtained by the three-dimensional analysis can be compared with the two-dimensional transient seepage analysis (Chen et al. 2005). The results show that the three-dimensional seepage occurs more rapidly than the two-dimensional seepage. In the present three-dimensional analysis, the perched water table in the cross section reaches the riverbed in 4.5 days. In the two-dimensional analysis, it took 5.0 days for the perched water table to reach the riverbed.

The evolution of total head contours and velocity vectors with time in the cross section at z = 150 m is shown in Fig. 8. The pattern of the total head distributions does not change significantly before the perched water table merges with the groundwater table (Figs. 8*a*, 8*b*). After the perched water table merges with the groundwater table in the riverbed, a flow channel forms. The flow rate increases abruptly because the coefficient of permeability of the soil in the flow channel and the flow velocities in the flow channel are much larger than those in the unsaturated zone.

Figure 9 shows the evolution of the pore-water pressure surfaces in the horizontal section at y = 50 m for case I. The wetting front with zero pore-water pressure advances from the upstream slope to the downstream slope with time. The pore-water pressures increase from the upstream surface to a maximum and then decrease to zero at the wetting front. The pore-water pressure gradients are larger near the abutment boundaries than in the middle part of the dam. Since the elevation in the section is a constant, the pore-water pressure gradients are actually the hydraulic gradients times the unit weight of water. Therefore, Fig. 9 also suggests that the hydraulic gradients are larger near the abutment boundaries

Fig. 6. Evolution of the phreatic surface in the dam for case I (homogeneous): (*a*) t = 2 days; (*b*) t = 4.5 days; (*c*) t = 6.5 days; (*d*) t = 9 days.

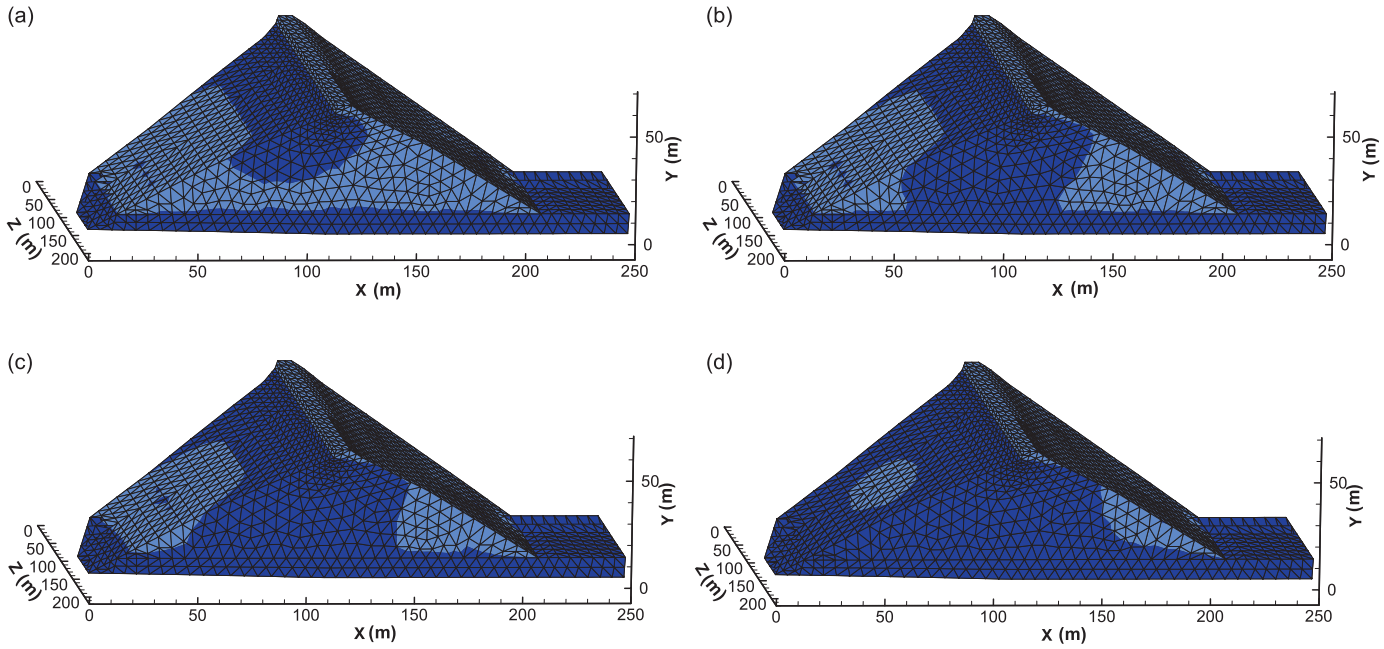

Fig. 7. Pore-water pressure contours (kPa) within the cross section at z = 150 m at different times for case I (homogeneous): (*a*) t = 2 days; (*b*) t = 4.5 days; (*c*) t = 6.5 days; (*d*) t = 9 days.

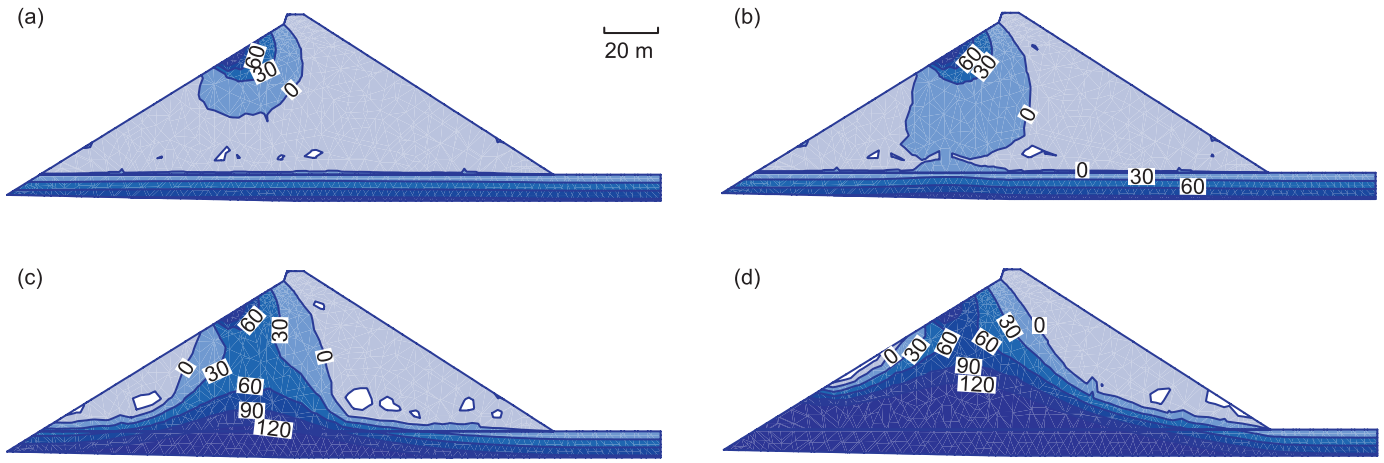

than in the middle part of the dam and that the abutment boundaries are more susceptible to internal erosion. The two-dimensional seepage analysis could not show these characteristics because only a cross section can be analyzed.

The pore-water pressure contours on the longitudinal section at x = 111.56 m at different times in case I are shown in Fig. 10. In Fig. 10*a*, the upper perched water zone is between the two zero pore pressure contours. The perched water flows faster along the abutment boundaries, and the pore-water pressures are larger at the abutment boundaries. In Fig. 10*b*, the perched water table has merged with the initial groundwater table at the side boundaries, and an occluded unsaturated zone in the lower middle part of the dam still remains. This again indicates that the wetting front near the abutment boundary advances faster than that away from the boundary. From Figs. 9 and 10, the abutment boundary of the dam is at a higher risk when water infiltrates into the dam. Not surprisingly, the onset of seepage failures in several dams, such as Teton dam, Clear Branch Dam, East Branch Dam, and Navajo Dam, occurred from erosion at the abutments (USCOLD 1988). When the perched water table reaches the riverbed after 4.5 days, the soils in the longitudinal section become saturated, and the flow pattern approaches steady-state conditions (Fig. 10*d*). The flow pattern in Fig. 10*d* was also shown in the three-dimensional steady-state seepage analysis of a uniform dam conducted by Freeze (1971).

The faster seepage flow near the impermeable abutment boundary can be explained by the boundary conditions. As water flows from the upstream to the downstream, the flow

Fig. 8. Total head contours (m) and velocity vectors within the cross section at z = 150 m at different times for case I (homogeneous): (*a*) t = 2 days; (*b*) t = 4.5 days; (*c*) t = 6.5 days; (*d*) t = 9 days.

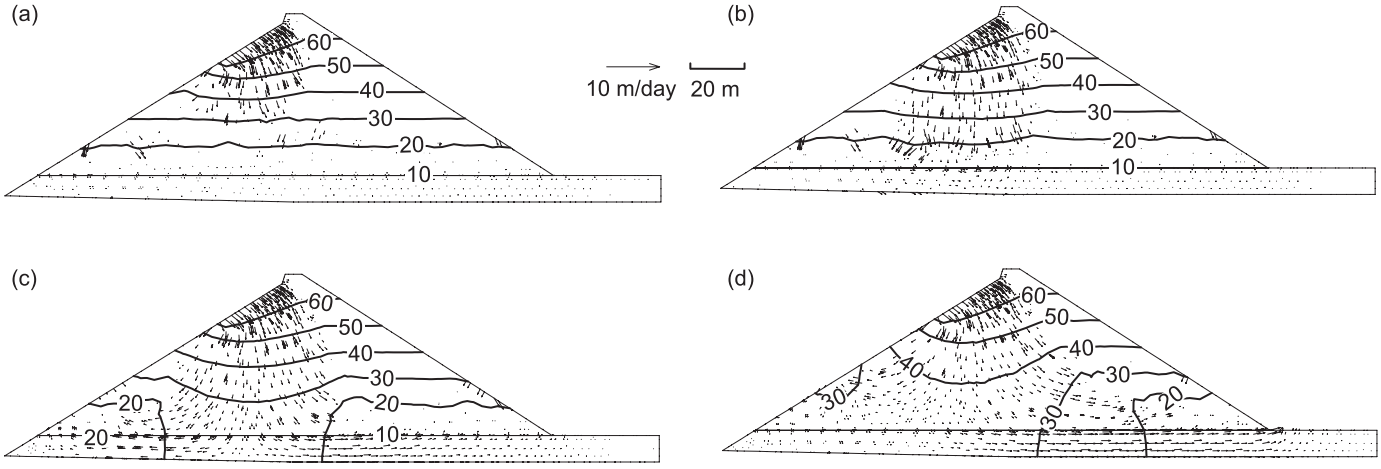

Fig. 9. Pore-water pressure surfaces within the horizontal section at y = 50 m at different times for case I (homogeneous): (*a*) t = 2 days; (*b*) t = 4.5 days; (*c*) t = 6.5 days; (*d*) t = 9 days.

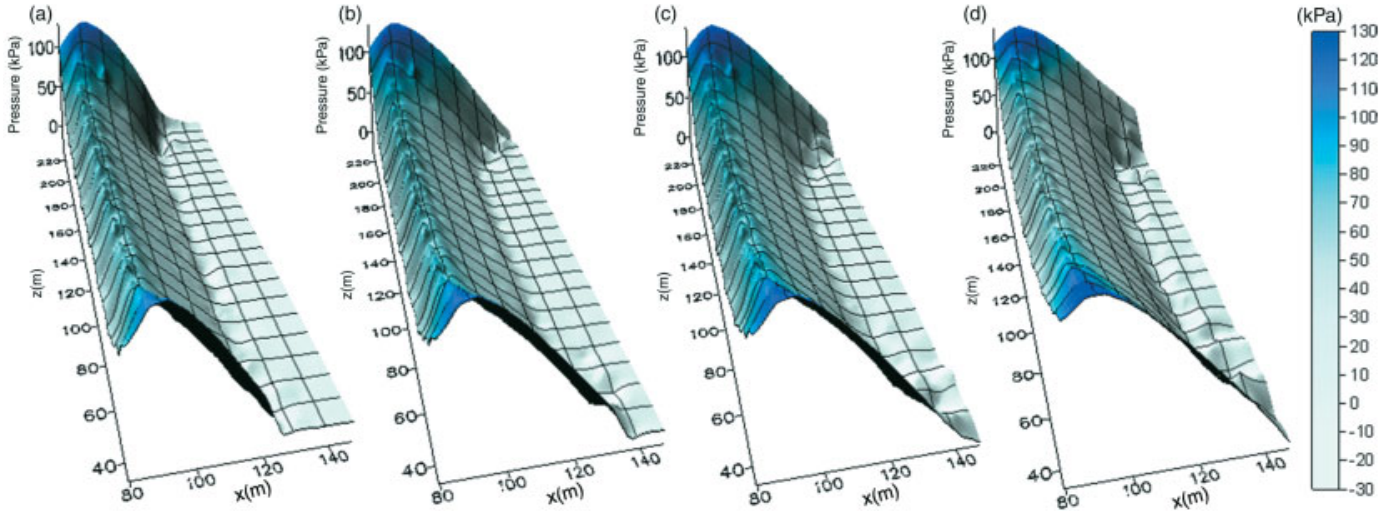

Fig. 10. Pressure contours (kPa) within the longitudinal section at x = 111.56 m at different times for case I (homogeneous): (*a*) t = 2 days; (*b*) t = 4.5 days; (*c*) t = 6.5 days; (*d*) t = 9 days.

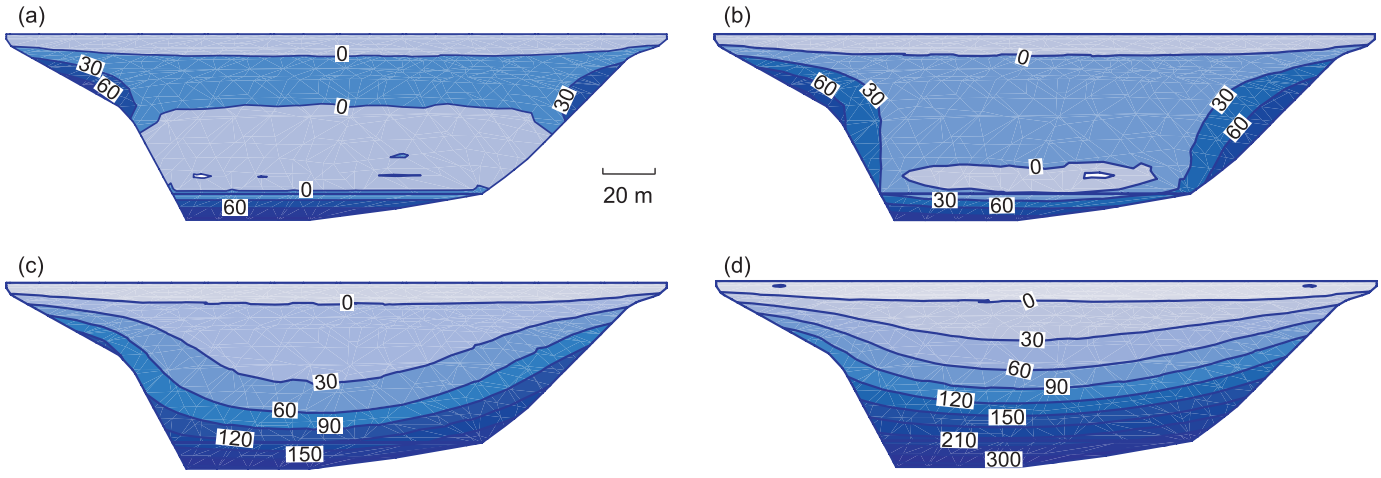

Fig. 11. Evolution of the phreatic surface in the dam, where it was assumed that $k_x = k_z = 2k_y$ (anisotropic): (*a*) t = 1 day; (*b*) t = 2.25 days; (*c*) t = 3.25 days; (*d*) t = 4.5 days.

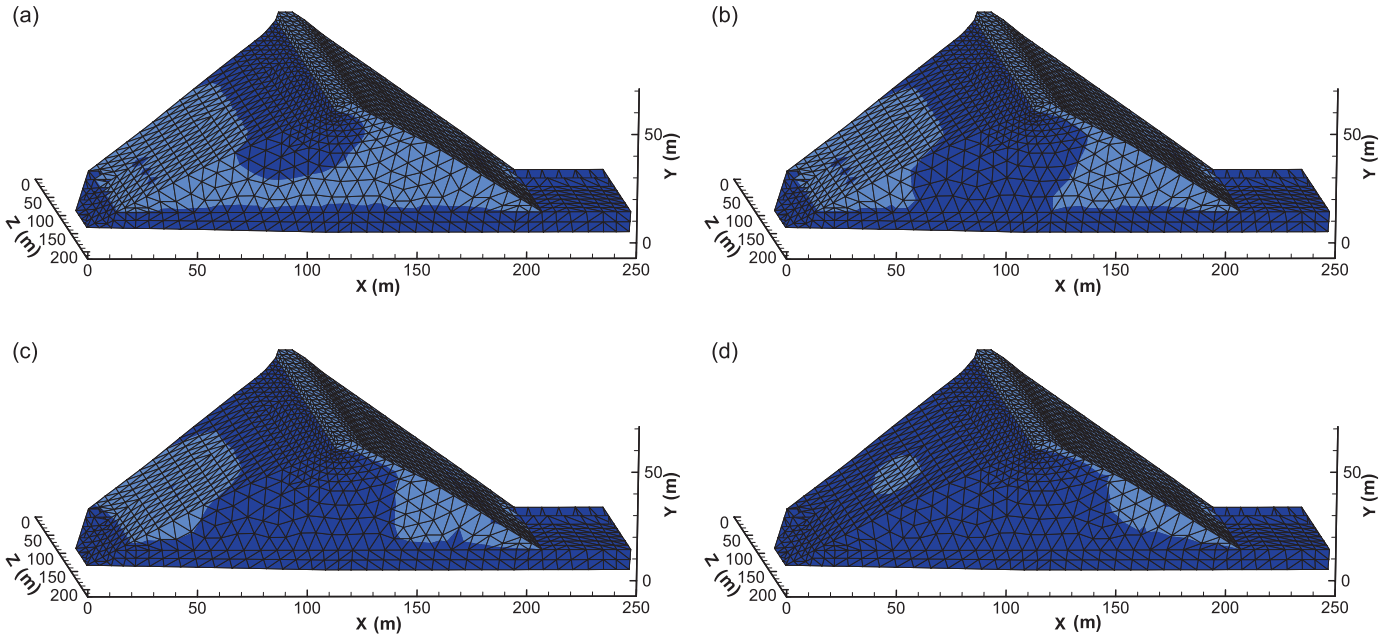

Fig. 12. Evolution of the phreatic surface in the dam for case II (sandwich layer): (*a*) t = 0.04 days; (*b*) t = 0.1 days; (*c*) t = 0.2 days; (*d*) t = 0.4 days.

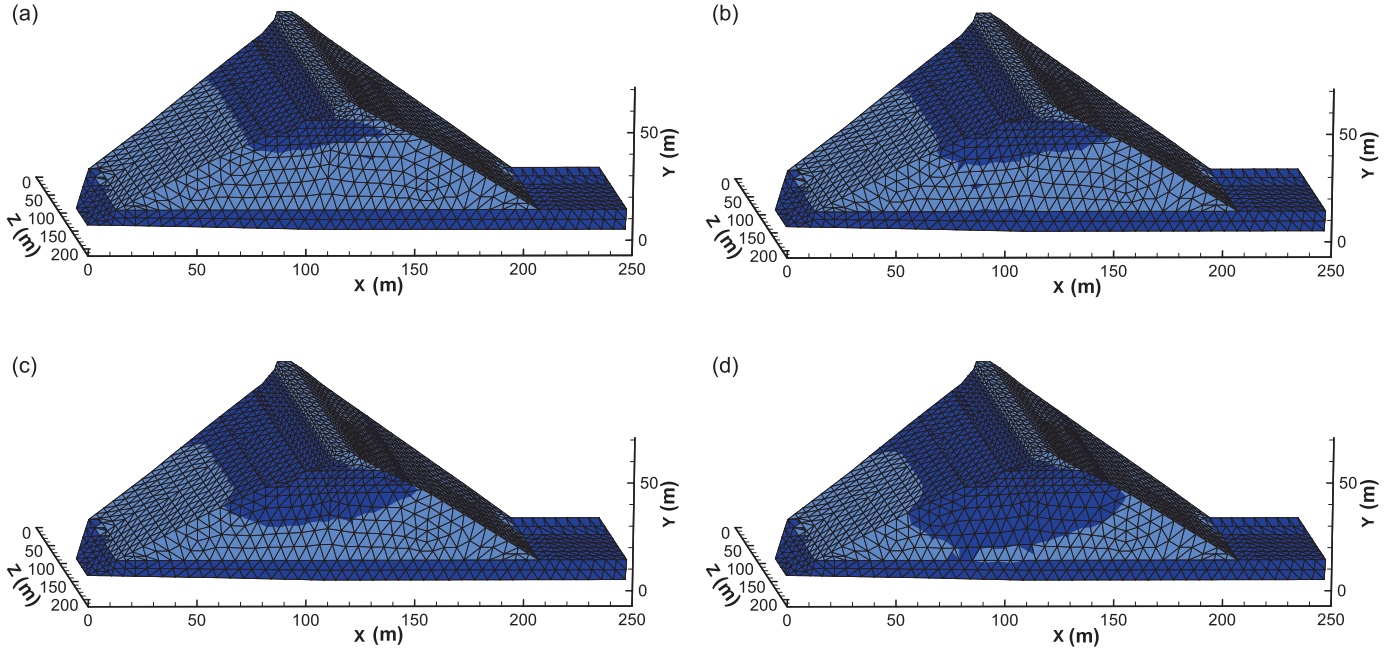

channel becomes narrower due to the geometry of the abutment boundaries. The zero-flux boundary condition requires that the normal flow velocity at the boundary be zero. To maintain the mass conservation requirement, the tangential velocity along the boundary must be larger. As such, the wetting front near the abutment boundaries advances faster. Since the abutment boundary effect cannot be considered in a two-dimensional analysis, the results obtained from the two-dimensional analysis underestimate the rate of wetting front advancement and do not reveal the risk of seepage failure near the abutment boundaries.

Effect of material anisotropy

To study the effect of anisotropy of the rockfill, a modification to case I was conducted in which the horizontal saturated coefficients of permeability k_x and k_z were assumed to

Fig. 13. Pore-water pressure contours (kPa) within the cross section at z = 150 m at different times for case II (sandwich layer): (*a*) t = 0.04 days; (*b*) t = 0.1 days; (*c*) t = 0.2 days; (*d*) t = 0.4 days.

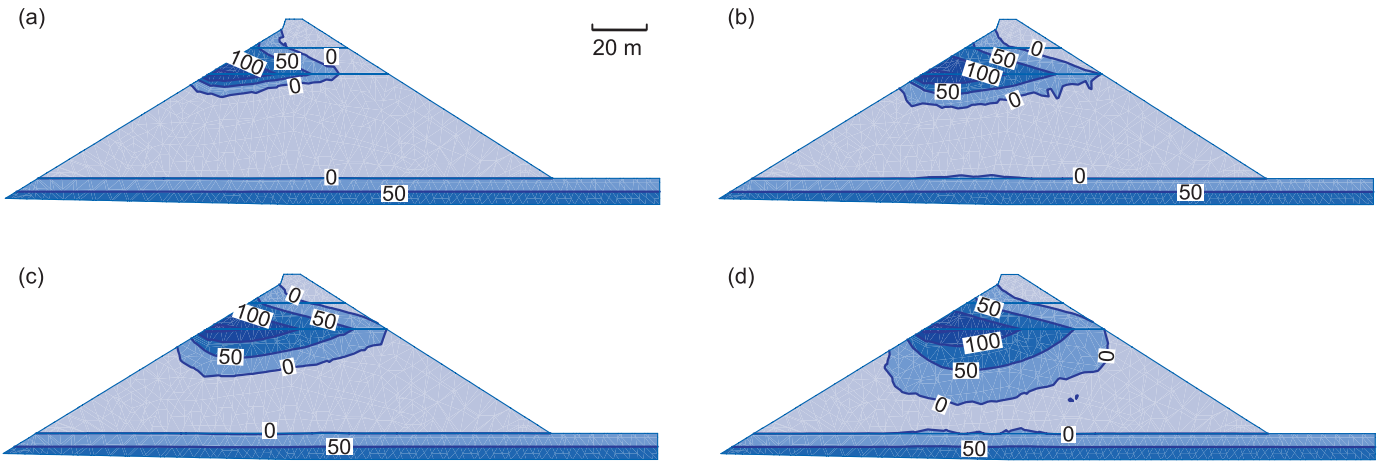

Fig. 14. Total head contours (m) and velocity vectors within the cross section at z = 150 m at different times for case II (sandwich layer): (*a*) t = 0.04 days; (*b*) t = 0.1 days; (*c*) t = 0.2 days; (*d*) t = 0.4 days.

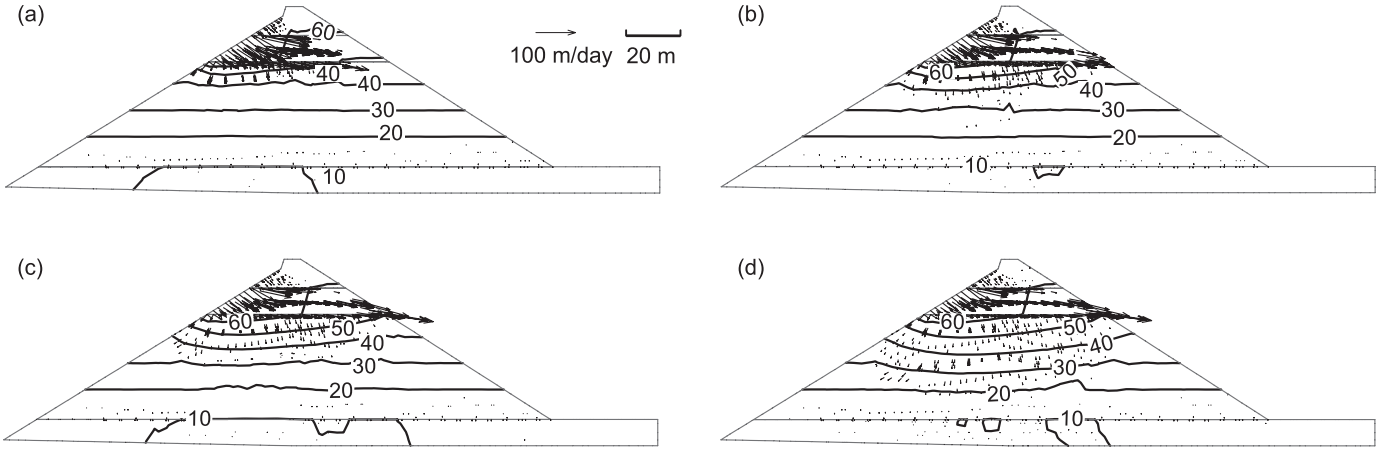

be twice the vertical saturated coefficient of permeability k_y. The vertical saturated coefficient of permeability remained the same. The evolution of the transient phreatic surface in the dam is shown in Fig. 11. The pattern of the reservoir water infiltration into the anisotropic rockfill is similar to that of reservoir water into the isotropic rockfill shown in Fig. 6. The infiltration velocity in the case of the anisotropic rockfill is approximately twice that in the case of the isotropic rockfill. In other words, it takes about half the time for the phreatic surface to reach the riverbed when the horizontal saturated coefficient of permeability is doubled. The anisotropy of the rockfill does not change the seepage mode of the dam but only accelerates the infiltration process.

Effect of stratification in rockfill

To consider segregation of the rockfill particles during construction, a coarse sandwich layer between elevations 3260 and 3270 m was assumed in the dam in case II. The lower limit of the grain-size distribution of the rockfill (Fig. 3) was adopted for the sandwich layer, and the average grain-size distribution was used for the rockfill. As a result, the sandwich layer is coarser than the rest of the rockfill.

Figure 12 shows the evolution of the phreatic surface in the dam for case II. Figure 13 shows the pore-water pressure contours within the cross section at z = 150 m at different times. Compared with Figs. 6 and 7, the advancement of the wetting front in case II differs considerably from that in case I. The wetting front advances primarily along the horizontal interface between the sandwich layer and the rockfill, which is consistent with the two-dimensional seepage results. After 0.1 days, the wetting front reaches the downstream slope surface as shown in Fig. 13*b*, which is shorter than the 0.15 days in the two-dimensional analysis. The wetting front has not reached the initial groundwater table, however, even after 0.4 days. This validates the phenomenon observed in the field, that is, before the dam was breached, the seepage water exited from the downstream slope surface near the high elevation of 3260 m, whereas no abnormal water flow was observed earlier in the riverbed. In other words, rockfill stratification might have played a key role in the seepage failure of the dam.

Fig. 15. Pore-water pressure surfaces within the horizontal section at y = 50 m at different times for case II (sandwich layer): (*a*) t = 0.04 days; (*b*) t = 0.1 days; (*c*) t = 0.4 days.

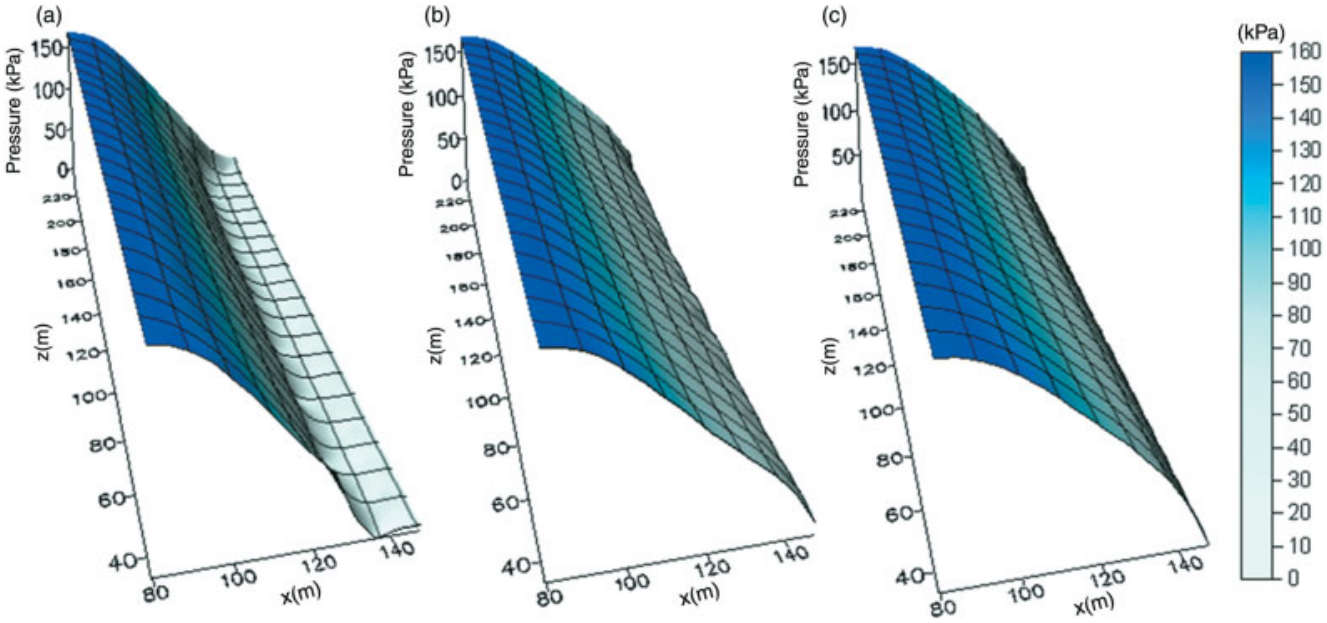

Fig. 16. Pore-water pressure contours (kPa) within the longitudinal section at x = 111.56 m at different times for case II (sandwich layer): (*a*) t = 0.04 days; (*b*) t = 0.1 days; (*c*) t = 0.2 days; (*d*) t = 0.4 days.

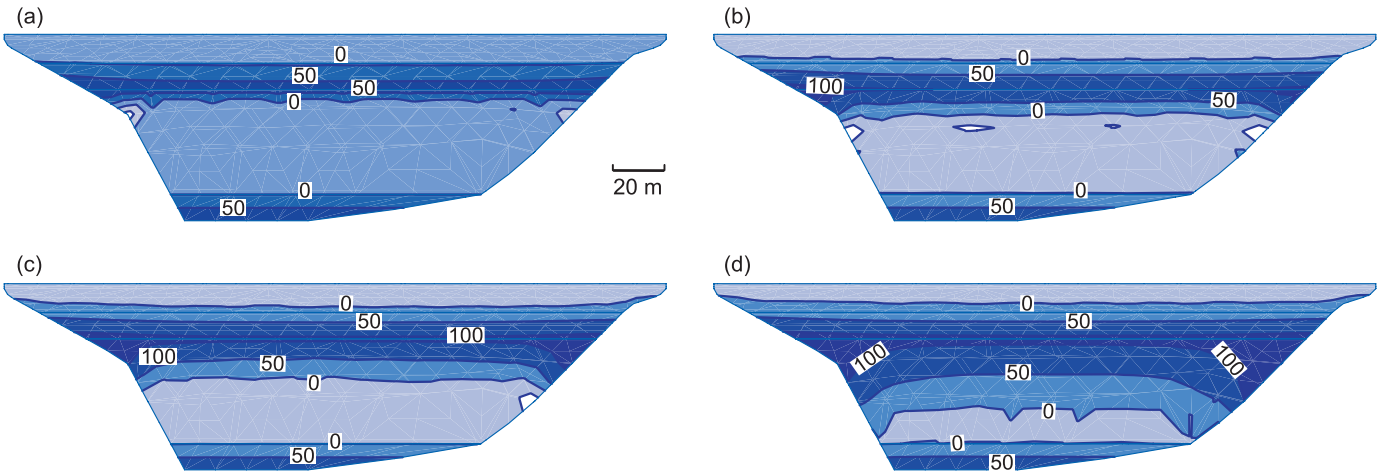

The total head contours and velocity vectors within the cross section at z = 150 m at different times obtained in case II are shown in Fig. 14. The contours become denser and the hydraulic gradients higher near the perched water table. The total head contours become nearly vertical and the flow direction becomes nearly horizontal inside the coarse sandwich. Therefore, horizontal seepage failure can be initiated along the sandwich layer.

The pore-water pressure surfaces in the horizontal section at y = 50 m (elevation 3260 m) at different times in case II are shown in Fig. 15. Before 0.1 days, the wetting front moves from the upstream slope surface towards the downstream. The differences in the pore-water pressures close to the abutment boundaries and in the middle part of the dam are smaller than those in case I. After 0.1 days, the pore-water pressures in the horizontal section change little with time.

Figure 16 shows the pore-water pressure contours in the longitudinal section at x = 111.56 m at different times in case II. The area between the two zero pore-water pressure contours is the wetted zone. The wetting front advances gradually downwards, and the perched water table nearly reaches the riverbed after 0.4 days at the abutment boundaries, long after the wetting front reaches the downstream slope at t = 0.1 days (Fig. 13*b*). The middle part of the dam, however, remains unsaturated even at t = 0.4 days (Fig. 16*d*). This is different from the seepage pattern shown for the uniform dam (Fig. 10) where the dominant flow direction is downwards.

Conclusions

Three-dimensional transient infiltration in the Gouhou

concrete-faced rockfill dam was simulated using saturated–unsaturated seepage theory. The evolution of the wetting front along each of the three dimensions was illustrated by pore-water pressure contours at different times.

According to the results of the three-dimensional seepage analysis, the three-dimensional geometry has a considerable effect on the infiltration characteristics of the dam. The infiltration velocities are not uniform in the longitudinal direction. Given the same material properties, the seepage flow in the three-dimensional analysis is faster than that in a two-dimensional analysis. The flow pattern in the maximum cross section from the three-dimensional analysis is similar to that from the two-dimensional analysis, however.

In the three-dimensional analysis, the pore-water pressure gradients near the abutment boundaries are higher than those in the middle part of the dam, and the wetting front near the abutment boundaries advances faster than that away from the boundary. Therefore, the abutment boundaries of the dam are at a higher risk of seepage failure when the reservoir water infiltrates into the dam. Not surprisingly, the onset of seepage failures in some dams occurred from erosion at the abutments. Since the abutment boundary effect cannot be considered in a two-dimensional seepage analysis, the results obtained from the two-dimensional analysis would underestimate the rate of wetting front advancement and the risk of seepage failure near the abutment boundaries.

The anisotropy of the rockfill material does not change the seepage failure mode of the dam but only alters the infiltration rate. Doubling the horizontal coefficient of permeability of the rockfill approximately doubles the infiltration velocity.

The seepage flow pattern is significantly affected by material stratifications. If the rockfill is uniform, the wetting front will advance downwards towards the riverbed and merge with the initial groundwater table. If there is a coarse sandwich layer in the dam, the wetting front will advance primarily along the interface between the sandwich layer and the rockfill and form a nearly horizontal flow channel in the sandwich layer. Seepage failure can be triggered in the sandwich layer when the infiltrated water exits from the downstream slope.

Acknowledgements

This research was substantially supported by a grant from the NSFC/RGC Joint Research Scheme between the National Natural Science Foundation of China and the Research Grants Council of the Hong Kong SAR (project N-HKUST611/03).

References

Aral, M.M., and Maslia, M.L. 1983. Unsteady seepage analysis of Wallace Dam. Journal of Hydraulic Engineering, **109**(6): 809–826.

Bathe, K.J., and Khoshagoftaar, M.R. 1979. Finite element free surface seepage analysis without mesh iteration. International Journal for Numerical and Analytical Methods in Geomechanics, **3**(1): 13–22.

Chang, C.S. 1987. Boundary element method in drawdown seepage analysis for earth dams. Journal of Computing in Civil Engineering, **1**(2): 83–98.

Chen, Z.Y., and Zhao, Y.Z. 1996. Slope stability study of the Gouhou Dam. Qinghai Water Power, Xining, China, **15**(1): 37–42.

Chen, Q., Zhang, L.M., and Zhu, F.Q. 2005. Effects of material stratification on the seepage field in a rockfill dam. *In* Proceedings of the 2nd Chinese National Symposium on Unsaturated Soils, Hangzhou, China, 23–24 April 2005. Chinese Soil Mechanics and Geotechnical Engineering Society, Beijing, China. pp. 508–515.

Desai, C.S. 1972. Seepage analysis of banks under drawdown. Journal of the Soil Mechanics and Foundations Engineering Division, ASCE, **98**(1): 1143–1162.

Dvinoff, A.H., and Harr, M.E. 1971. Phreatic surface location after drawdown. Journal of the Soil Mechanics and Foundations Engineering Division, ASCE, **97**(1): 47–58.

Fell, R., MacGregor, P., and Stapledon, D. 1992. Geotechnical engineering of embankment dams. A.A. Balkema, Rotterdam, The Netherlands.

Foster, M., Fell, R., and Spannagle, M. 2002. The statistics of embankment dam failures and accidents. Canadian Geotechnical Journal, **37**: 1000–1024.

Fredlund, D.G., and Morgenstern, N.R. 1977. Stress state variables for unsaturated soils. Journal of the Geotechnical Engineering Division, ASCE, **103**(5): 447–466.

Fredlund, D.G., and Rahardjo, H. 1993. Soil mechanics for unsaturated soils. John Wiley & Sons, Inc., New York.

Fredlund, D.G., Xing, A., and Huang, S. 1994. Predicting the permeability function for unsaturated soils using the soil-water characteristic curve. Canadian Geotechnical Journal, **31**: 533–546.

Fredlund, M.D., Wilson, G.W., and Fredlund, D.G. 2002. Use of the grain-size distribution for estimation of the soil-water characteristic curve. Canadian Geotechnical Journal, **39**: 1103–1117.

Freeze, R.A. 1971. Influence of the unsaturated flow domain on seepage through earth dams. Water Resources Research, **7**(4): 929–941.

Gouhou Dam Failure Investigation Team. 1996. Technical details of the Gouhou Dam. *In* Gouhou concrete-faced rockfill dam — design, construction, operation, and failure. *Edited by* China National Flood and Drought Prevention Office. Water Conservancy and Hydropower Press, Beijing, China. pp. 111–245.

Gupta, C.S., Bruch, J.C., Jr., and Comincioli, V. 1986. Three-dimensional unsteady seepage through an earth dam with accretion. Engineering Computations (Swansea, Wales), **3**(1): 2–10.

Lam, L., Fredlund, D.G., and Barbour, S.L. 1987. Transient seepage model for saturated–unsaturated soil systems: a geotechnical engineering approach. Canadian Geotechnical Journal, **24**: 565–580.

Liu, J., and Miao, L.J. 1996. Experimental study of seepage and seepage stability of Gouhou rockfill materials. *In* Gouhou concrete-faced rockfill dam — design, construction, operation, and failure. *Edited by* China National Flood and Drought Prevention Office. Water Conservancy and Hydropower Press, Beijing, China. pp. 18–25.

Liu, J., Ding, L.Q., Miao, L.J., and Yang, K.H. 1998. Model study on failure mechanisms of the Gouhou rockfill dam. Chinese Journal of Hydraulic Engineering, Beijing, **29**(11): 69–75.

Neuman, S.P. 1972. Saturated–unsaturated seepage by finite elements. Journal of the Hydraulics Division, ASCE, **99**(12): 2233–2250.

Ng, K.L.A., and Small, J.C. 1995. Simulation of dams constructed with unsaturated fills during construction and impounding. *In* Unsaturated soils. *Edited by* E.E. Alonso and P. Delage. A.A. Balkema, Rotterdam, The Netherlands. pp. 281–286.

Ng, C.W.W., Wang, B., and Tung, Y.K. 2001. Three-dimensional numerical investigations of groundwater responses in an unsaturated slope subjected to various rainfall patterns. Canadian Geotechnical Journal, **38**: 1049–1062.

PDE Solutions Inc. 2003. FlexPDE 3 reference manual. PDE Solutions Inc., Antioch, Calif.

Russo, D., Zaidel, J., and Laufer, A. 1998. Numerical analysis of flow and transport in a three-dimensional partially saturated heterogeneous soil. Water Resources Research, **34**(6): 1451–1468.

Singh, B., and Varshney, R.S. 1995. Engineering for embankment dams. A.A. Balkema, Brookfield, Vt.

SoilVision Systems Ltd. 2003. SVFlux user manual 3.12, saturated/unsaturated finite element 2D/3D seepage modeling. SoilVision Systems Ltd., Saskatoon, Sask.

USCOLD. 1988. Lessons from dam incidents. USA-II. Subcommittee of Dam Incidents and Accidents, Committee on Dam Safety, U.S. Committee on Large Dams (USCOLD), American Society of Civil Engineers (ASCE), New York.

Xie, H.Q., He, J.D., Zhang, J.H., and Xie, J.Q. 2001. 3D seepage flow characteristics in the right bank of the Zipingpu project. Journal of Sichuan University (Engineering Science Edition), Chengdu, China, **33**(6): 10–13.

Zhou, Q.Y., Shimada, J., and Sato, A. 2002. Temporal variations of the three-dimensional rainfall infiltration process in heterogeneous soil. Water Resources Research, **38**(4): 1-1–1-16.